

Real-Time In Situ Holographic Optogenetics Confocally Unraveled Sculpting Microscopy

Gilad M. Lerman, Justin P. Little, Jonathan V. Gill, Dmitry Rinberg, and Shy Shoham*

Two-photon (2P) optogenetic stimulation is currently the only method for precise, fast, and non-invasive cellular excitation deep inside brain tissue; it is typically combined with holographic wavefront-shaping techniques to generate distributed light patterns and target them to multiple specific cells in the brain. During propagation in the brain, these light patterns undergo severe distortion, mainly due to scattering, which leads to a discrepancy between the desired and actual light distribution. However, despite its importance, measurement of these tissue-induced distortions and their effects on the light patterns has yet to be demonstrated in situ. To this end, holographic optogenetics confocally unraveled sculpting (HOCUS), a system for real-time in situ evaluation of holographic light patterns, based on confocally descanning the stimulation light's reflection from the brain, is developed. HOCUS measures both tissue and wave propagation properties and enables the real-time measurement and correction of the dimensions and positions of holographic spots relative to neurons targeted for stimulation. It can also be used to measure tissue attenuation length, and thus should facilitate future attempts to optimize the generated hologram to pre-compensate for tissue-induced distortions, thereby improving the reliability of 2P holographic stimulation experiments.

light modulators (SLMs).^[3,5,6,8–12] These patterns are frequently composed of cell soma sized “spots,” which are focused up to a few hundred micrometers deep into the brain to stimulate specific pre-chosen neurons with high temporal precision.^[13,14]

A few factors influence the intensity distribution at the focal plane and cause a discrepancy between the desired and the actual result. As these light patterns propagate in brain tissue toward the focal plane, they experience extensive scattering and are subject to complex, unpredictable distortions that must be estimated and compensated for. In the context of wavefront-shaped holographic^[8,15] or spatiotemporal^[9,16] focusing applications, prediction of the final light distribution becomes even harder due to the difficulty of combining wave-based and scattering-related calculations during hologram generation. In addition, the intensity of holographically generated spots is generally not uniform due to,

among other factors, position-dependent diffraction efficiency of the SLM and optical aberrations and needs to be corrected with a relevant spatial correction function.

These concerns are usually treated either theoretically, based on elaborate computational effort,^[17,18] or experimentally based on direct measurements using brain slices.^[19] During the design of a new holographic optogenetic targeting technique, correction functions are implemented in the process of hologram generation and the method is calibrated and validated experimentally. Nevertheless, the nature and complexity of these experiments prevent them from being carried out prior to every stimulation experiment, and a method for in situ measurements of the tissue-induced distortions and holographically generated light pattern fidelity is yet to be demonstrated. The user, therefore, must rely solely on the robustness and stable calibration of the targeting method despite the natural variations in experiments and time.

To directly address these issues, we developed a method for real-time in situ evaluation of the tissue-induced distortions of the holographic light patterns, permitting measurement of the dimensions and positions of the pattern relative to neurons targeted for stimulation. The method is based on confocally descanning the reflection of the holographic light patterns focused into the brain. By measuring the unique tissue-induced distortions of the specific animal and holographic pattern to be used

1. Introduction

Two-photon (2P) optogenetic stimulation provides spatially precise cellular level stimulation by minimizing out-of-focus neuron excitation, often in combination with complementary techniques like temporal focusing and soma-restricted opsin expression.^[1–7] To stimulate multiple neurons, distributed holographic light patterns can be generated and dynamically controlled using spatial

Dr. G. M. Lerman, Dr. J. P. Little, Prof. S. Shoham
Neuroscience Institute
Tech4Health Institute
Department of Ophthalmology
NYU Langone Health
New York, NY 10016, USA
E-mail: shoham@nyu.edu

J. V. Gill, Prof. D. Rinberg
Center for Neural Science
New York University
Neuroscience Institute
NYU Langone Health
New York, NY 10016, USA

 The ORCID identification number(s) for the author(s) of this article can be found under <https://doi.org/10.1002/lpor.201900144>

DOI: 10.1002/lpor.201900144

in an immediate photostimulation experiment, this method enables real-time correction of the positions of holographic spots and can potentially be used to optimize the generated hologram to compensate for tissue-induced distortions. This may significantly improve the reproducibility of 2P holographic stimulation experiments, especially in live, awake animals. Tissue properties such as attenuation length due to scattering can be measured as well, making this method a relevant part of the toolkit used for tissue characterization.

Imaging by descanning light reflection takes advantage of a scanning excitation mechanism already present in the experimental apparatus, using it in the opposite direction to gain additional information about the sample. Photons emitted from the sample, due to ballistic reflections from the excitation source or fluorescence, are imaged with a confocal detection system. Previously, this approach has been used for long-wavelength reflectance imaging, in combination with a fluorescence imaging setup, using the reflections of the excitation light.^[20,21] In our setup, we use reflection of the 2P optogenetic stimulation laser and get additional information about its position, dimensions, and intensity distribution. **Figure 1a** shows a schematic of our descanning system.

2. System Design

The optical configuration of our system is presented in Figure 1b and is based on the concept of confocally descanning^[20,21] the stimulation light's reflection from the tissue, thereby reconstructing its shape and position. Our holographic optogenetics confocally unraveled sculpting (HOCUS) detection module is added onto an existing all-optical imaging and stimulation system described in detail^[22] elsewhere can, in principle, be added to any microscope with 2P optogenetic stimulation capabilities. The system combines an imaging arm with a 920 nm femtosecond (fs) laser illumination source (Spectra Physics, Insight X3), and a photostimulation arm with a 1028 nm fs amplified laser source (Light Conversion, Pharos). The holograms were calculated using custom MATLAB software that makes use of a modified Gerchberg–Saxton algorithm^[23] and were loaded onto the SLM (HSPDM512–920-1110, Meadowlark Optics, optimized for 1064 nm, 7.68 mm × 7.68 mm active area, 512 × 512 pixels).

Both stimulation and imaging beams are projected onto the brain and are back-reflected through the objective and along their original combined path. In order to separate the reflection of the stimulation light from the reflected imaging light, we used a polarization beam splitter (PBS) (Thorlabs, PBS253) to combine the imaging and stimulation arms, each linearly polarized orthogonally to the other arm. We added a quarter waveplate (QWP) (Thorlabs, AQWP10M-980) after the PBS so that the light reflected from the brain double-passes through the QWP and its polarization direction will be rotated by 90 degrees. This ensures that back-reflected stimulation light will pass through the PBS along the imaging light path, while the reflected imaging beam will be deflected away from this path. After the reflected stimulation light is descanned by the galvo-resonant mirror pair, it is reflected by a dichroic mirror (Semrock, FF989-SDi01-25 × 36) and separated from the incoming imaging light. The reflected stimulation light beam next hits an electrically tunable lens (ETL)

(Optotune, EL-10-30-TC) that focuses it onto a 10 μm diameter pinhole (Thorlabs, P10S). The ETL is used to fine tune the focused beam on the pinhole without the need to physically move the lens and allows to scan the imaging plane when 3D mapping the stimulation pattern. The role of the pinhole is twofold: it enables the point-by-point scan of the stimulation beam as it blocks the lateral out-of-focus light, and it enables the imaging of different planes in combination with the ETL as it blocks the axial out of focus light. The pinhole is thus essential to the detection of the weak reflected signals from the brain on top of the much stronger reflections from the transcranial window as it confocally rejects the out-of-focus signal.

The beam is re-collimated and refocused onto a detector (Thorlabs, APD410C) by a pair of lenses (Thorlabs, $f = 50.0$ mm, LA1131-C). This detector is an affordable, small form-factor solution for the near infrared regime with high sensitivity to capture the small signal of the light reflected from the brain. The signal from the detector is amplified (DHPCA-100, Femto), digitized, and captured using ScanImage (Vidrio Technologies).^[24] Subsequent image processing was limited to subtracting a constant noise pattern that originates from residual reflections of the incoming stimulation light on the PBS, and to weak image smoothing.

Ensuring precise, real-time cellular targeting requires the coregistration of three different fields of view (FOVs): the stimulation FOV, the imaging FOV, and the HOCUS FOV. For this coregistration, a calibration pattern was burned onto a fluorescent plate (Ted Pella, Inc.) by the photostimulation system. The plate was then imaged by the 2P imaging system and the calibration pattern was used for the registration of the two systems. In the next step, we removed the fluorescent plate and placed a mirror at the focal plane of the objective lens. The reflection of the calibration pattern was imaged by HOCUS and was used to register HOCUS FOV to the other FOVs. Figure 1 also shows proof-of-concept examples of HOCUS microscopic imaging of light patterns back-reflected from physical samples. The first is a five-spot stimulation pattern projected onto a glass cover slide (Figure 1c) positioned at the focal plane. The reflection from the glass is much stronger than the reflection from the brain tissue and there is no distortion due to scattering. The second is a spot imaged inside the mouse's implanted glass cranial window (Figure 1d). As can be seen, the spot is diffused and aberrated, and as a result the spot size increases while its intensity decreases. Since HOCUS can image these spot size changes and intensities, it can be used to measure the tissue scattering manifested as attenuation length and in principle also to compensate for optical aberrations by serving as the feedback in a closed loop process of iteratively reducing the spot size imaged by HOCUS.

3. Measurements and Results

To explore the in vivo performance of HOCUS, we injected the olfactory bulb of mice with a 1:1 mixture of viral vectors for the calcium indicator GCaMP6s and the redshifted opsin ChrimsonR, which respectively enable the imaging of the cell's activity and its photostimulation (AAV5-Syn-GCaMP6s-WPRE-SV40 and AAV5-Syn-ChrimsonR-tdTomato, UPENN vector core). All animal procedures were approved under a New York University

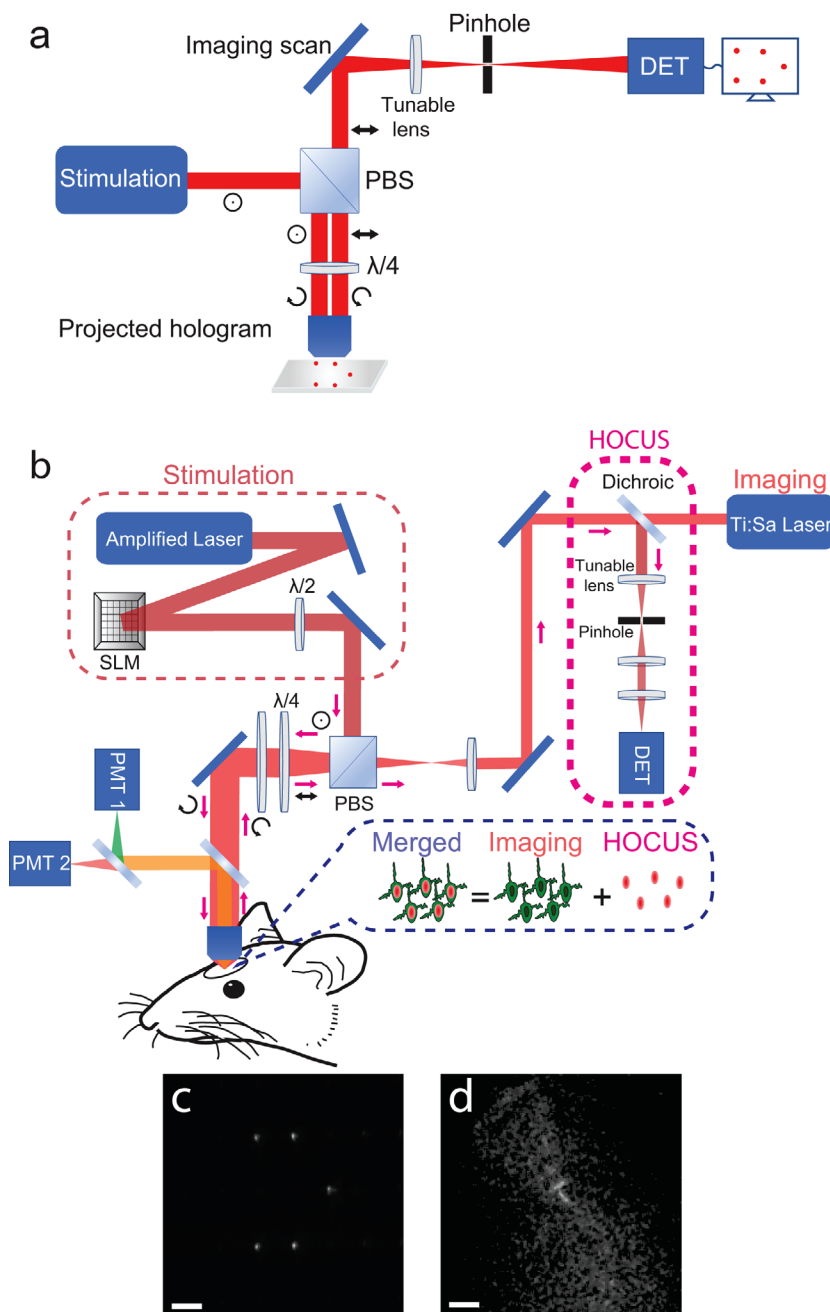


Figure 1. a) A schematic of the descanning system combining reflected stimulation light with confocal imaging shown with the polarization state at each stage. DET, detector. b) Experimental setup. The 2P imaging path is combined with the holographic 2P photostimulation path for in vivo experiments in head-fixed, behaving mice. The reflected stimulation light passes through the PBS, is descanned by the mirrors, and then reflected by the dichroic mirror through the pinhole onto the detector. PBS, polarizing beam splitter; PMT1, PMT2, photomultiplier tubes; SLM, spatial light modulator; DET, detector. c) HOCUS measurement of a five-spot stimulation pattern reflected from a glass sample. d) A sample of a spot inside the mouse's implanted glass cranial window showing the ability of HOCUS to measure optical aberrations. Scale bars: 25 μm .

Langone Health institutional animal care and use committee (IACUC) protocol 161211-02. Following injection, a cranial window was implanted, replacing a circular piece of skull by a glass coverslip (3 mm diameter, Warner Instruments) that was secured in place using a mix of self-curing resin (Orthojet, Lang Dental) and cyanoacrylate glue (Krazy Glue). Prior to every stimulation experiment, we used the green and red fluorescence

signals to choose cells that express both GCaMP6s and ChrimsonR, and then generate a pattern of circular patches that will cover these cells. Next, we projected the spots onto the brain and used HOCUS to image the reflection of these spots to estimate their shape and position. **Figure 2** shows a pattern of four light spots projected onto the brain, 120 μm deep in the olfactory bulb, and positioned on four respective neurons. This figure merges

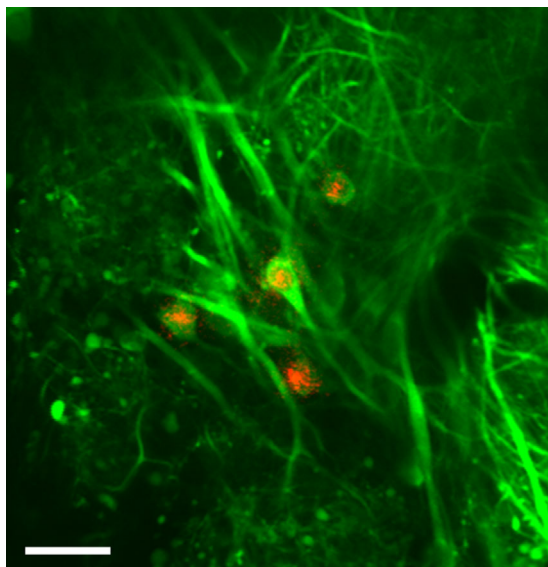


Figure 2. A merged image of GCaMP6s expression (green) and the HOCUS-imaged reflected stimulation light (red) showing a pattern of four light spots projected onto the brain, 120 μm deep in the olfactory bulb, and positioned on four respective neurons. Darker regions are caused by local vasculature. Scale bar: 25 μm .

the imaging channel showing the GCaMP6s signal (green) and the HOCUS channel showing the reflection of the stimulation pattern (red). The power levels used for the HOCUS imaging are kept low (<3 mW/cell) so that the stimulation pattern will not damage the cells even after a few minutes of exposure. We used galvo mirrors for the scan with a frame rate of one frame per second which can be further increased by improving the signal-to-noise ratio (SNR) of the system. After the position and shape of the stimulation pattern was verified by HOCUS and corrected if needed, the stimulation power was increased, and the photostimulation experiment began.

Although the scattering of near-infrared light in brain tissues is greatly reduced compared to that of visible light,^[25–27] it is still an important factor that needs to be considered when attempting 2P stimulation in deep layers. Scattering-related effects increase the spot size and reduce the intensity over the

targeted cells, effects that combine to compromise the excitation efficiency and specificity. To characterize the tissue-scattering effect, we generated and projected a hologram of a single (nearly) diffraction-limited light spot, which was z-scanned by moving the objective across different depths in the olfactory bulb. At each depth, we imaged both GCaMP6s fluorescence and the reflected stimulation light distribution with HOCUS (see Video S1, Supporting Information). Spot dimensions were estimated using a fit to a 2D Lorentzian function at each depth (Figure 3a) and were found to increase linearly for deeper penetration depths to >25 μm full width at half max (FWHM). Imaging was stopped at 320 μm (below the mitral cell layer), where the GCaMP6s signal was too weak to clearly discern cells, while the (strongly scattered) HOCUS signal was still visible. Interestingly, the spot dimensions on the upper side of the cranial glass window is just 2 μm (FWHM, red star), while its width at the lower side of the window at the brain's surface ($z = 0$) was 5 μm . It is well known that the transcranial glass window can introduce aberrations to the imaging and stimulation beams, degrading their performance.^[28] HOCUS can directly measure these aberrations and allows their correction by, for example, adjusting the objective's angle relative to the cover glass.

HOCUS can provide not only valuable information about the position and shape of the spots, but also about their relative intensities and the intensity uniformity within each spot, which can be used to optimize the 2P signal for stimulation. Figure 3b shows the attenuation of the maximum intensity of the spot (calculated as the average of 25 pixels in the center of the beam) as a function of penetration depth. The center of the beam comprises mainly ballistic photons arriving at the focal plane,^[26] while the beam attenuates with an attenuation length that is dependent on both scattering and absorption. At 1028 nm, absorption is negligible compared to scattering^[27] and so the attenuation length is dominated by scattering. As we use a pinhole to block the scattered light, the photons that reached the detector are ballistic photons that have travelled twice the penetration depth. From this measurement, we found an attenuation length of 229 μm at a wavelength of 1028 nm, which agrees well with previous measurements of attenuation lengths of 152–158 μm at 920 nm and 305–319 μm at 1300 nm.^[27,29]

We next generated large circular patch holograms (i.e., not diffraction-limited spots) of different sizes and projected them at

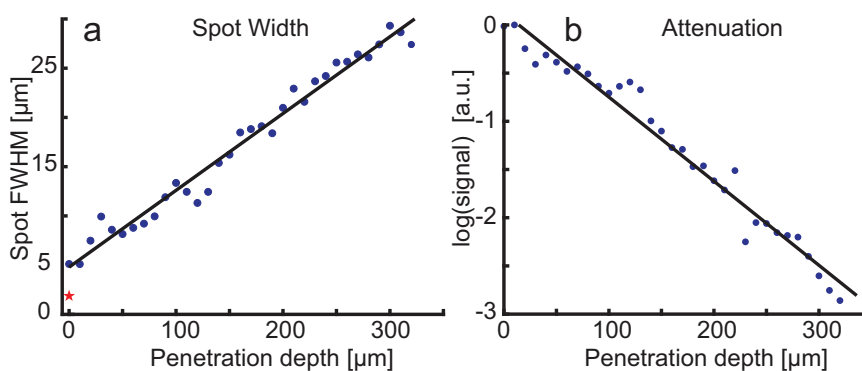


Figure 3. a) FWHM of the spot as a function of the penetration depth. The objective lens was scanned from the bottom surface of the glass window down to 330 μm deep, and the spot size was measured at every 10 μm . The red star shows the spot size on the upper side of the glass window. b) The maximum intensity of the spot at each penetration depth. This intensity decays exponentially with a decay length of 229 μm .

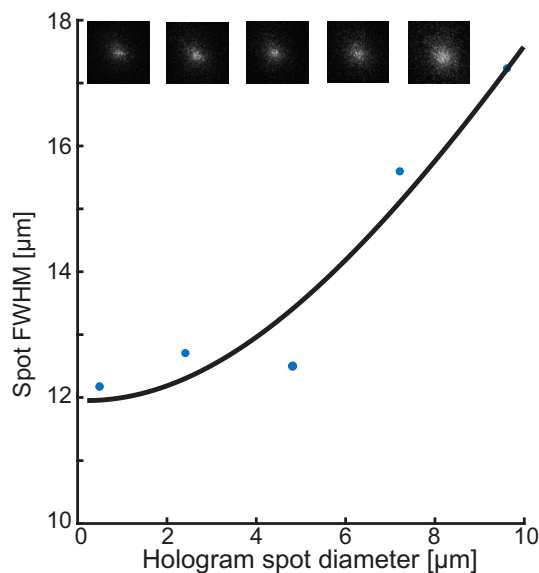


Figure 4. The FWHM of spots with different sizes measured at 100 μm deep as a function of the requested hologram spot diameter. The measured figures of all spots are shown in order at the top.

a depth of 100 μm in the olfactory bulb. The HOCUS images of these spots and their estimated dimensions (FWHM) are shown in **Figure 4**. At small values of the patch diameter, the measured spot's dimensions slowly increase as a function of the hologram dimension, but for larger values, the measured spot's dimensions increases much faster. As was shown in Figure 3a, for every depth, there is a natural scattering-related PSF for the HOCUS imaging system, which measures $\approx 13 \mu\text{m}$ FWHM at $z = 100 \mu\text{m}$. The HOCUS measurement is a convolution between this imaging PSF kernel and the actual spot. Therefore, the resulting width is given by $\sqrt{c^2 + ax^2}$ where c is the FWHM of the PSF kernel, x is the hologram spot diameter, and a is a multiplicative constant. At small values of hologram spot diameter x , the constant PSF kernel c is dominant and the change in measured spot width is slow. As the hologram spot diameter x increases, it becomes more dominant than the PSF kernel c and the measured spot size approaches a linear dependency on the change of hologram spot diameter.

The precise positioning of the light spots of the hologram is a crucial factor in the success potential of every cellular resolution optogenetic experiment. A deviation of a few μm can lead to activation of unwanted cells and to a misinterpretation of the neural circuit being investigated. Often, the holograms are misplaced

due to brain movements. These movements can occur after the hologram was already calculated, just before an experiment is about to start. To compensate for these movements, one can use a motion correction algorithm^[30] that tries to iteratively bring the FOV back to its original position by comparing it to a reference image. These algorithms greatly depend on the current state of the FOV; that is, if the imaging has degraded due to bleaching of the fluorescent molecule or brain plasticity, it will affect the accuracy of the algorithm leading to a misplaced FOV or to a non-converging iteration process. Dealing with brain movements is another advantage of HOCUS as it allows real-time imaging of the position of the spots while still using the fluorescence channel to image the cells. While imaging the FOV, we can change the hologram in real-time by adding a periodic phase pattern to the current hologram on the SLM. This periodic phase acts as a diffraction grating by moving the spots in a desirable distance and direction. This method is immediate as it does not require the recalculation of a new hologram from scratch, and the results of adding the additional grating phases are instantly seen with HOCUS, allowing a user to “walk” the spot step-by-step to cover the cell. **Figure 5a–d** shows a process of repositioning a spot on a cell by adding phases of gratings to its original hologram. The full movement of this spot is shown in Video S2, Supporting Information. This method enables quick corrections and fine tuning of the hologram, applied just before the stimulation experiment is carried out. We anticipate that SNR improvement will allow real-time motion correction during experiments.

HOCUS subsystems can be added to most conventional all-optical imaging and stimulation systems, and we anticipate it will be routinely used in such experiments. Our optical design was inspired by the back-scatter descanning arms added to multiphoton microscopes for observing intrinsic contrast signals from axonal structures,^[20,21] and can be easily modified to also allow their observation.

Additional improvement can be achieved by removing the background noise arising from residual reflections from the PBS by using a PBS with no residual reflection to unwanted directions, or by adding an additional polarizer to the HOCUS path before the ETL. As well, following Xia et al.^[21] the QWP can be replaced by a QWP cover-slip to further minimize the background reflection signal. Estimating the 2P signal based on HOCUS measurements requires some caution, since due to scattering, photons at the outskirts of the spot arrive at the focal plane with different times than photons at the center of the spot. This temporal discrepancy translates into a reduced 2P signal, and therefore, the actual 2P spot size for stimulation would be smaller than just the square of the HOCUS signal.

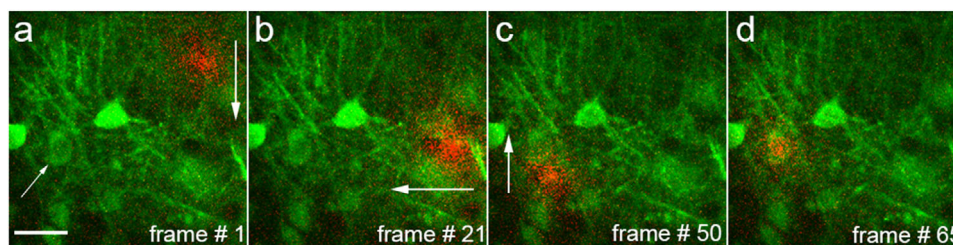


Figure 5. a–d) Walking the spot in the FOV toward the chosen cell by adding phases of gratings to its original hologram. Scale bar: 20 μm . The diagonal arrow on panel (a) shows the target cell and all the straight arrows in all panels show the direction of spot movement.

To summarize, in order to address the discrepancy between the desired and actual 2P holographic light pattern, we have developed a real-time method for evaluating the dimension, position, and intensity distribution of holographic patterns in situ. Based on confocally descanning the reflection of the stimulation light pattern we can reconstruct the stimulation pattern, assess its similarity to the desired pattern, and correct its position in a straightforward manner. In addition, a direct measurement of light distribution in the brain allows for better estimation and modeling of the temperature rise due to stimulation. The thermal effects caused by stimulation are usually neglected but are becoming more dominant with the increase of the number of stimulated cells and stimulation duration. Mapping in situ light distribution can thus help in estimating the temperature and designing better targeting methods for dealing with dangerous thermal effects.^[31,32] Our HOCUS depth-imaging attenuation estimate agrees nicely with independently measured tissue scattering coefficients. In the future, this method could potentially be used as a ground truth feedback for the iterative calculation of holograms, enabling a closed loop that will help optimize the holograms used for stimulation. The new method adds an additional level of reliability to 2P holographic stimulation experiments by verifying that the holographic projections are as desired, thereby improving their reproducibility and efficiency.

Supporting Information

Supporting Information is available from the Wiley Online Library or from the author.

Acknowledgements

The authors thank S. Rosen and B. Migliori for comments on the manuscript. This work was supported by the NIH BRAIN Initiative Grants (1U01NS090498-01) and U19 NS107464-01. J.G. was supported by the NIH graduate training grant (T90DA043219).

Conflict of Interest

G.L. and S.S. are inventors for a patent application on HOCUS.

Keywords

holography, light shaping, optogenetics, two-photon photostimulation

Received: April 29, 2019

Revised: June 17, 2019

Published online: August 13, 2019

[1] J. P. Rickgauer, D. W. Tank, *Proc. Natl. Acad. Sci. USA* **2009**, *106*, 15025.

- [2] V. Emiliani, A. E. Cohen, K. Deisseroth, M. Hausser, *J. Neurosci.* **2015**, *35*, 13917.
- [3] A. M. Packer, L. E. Russell, H. W. Dalgleish, M. Hausser, *Nat. Methods* **2015**, *12*, 140.
- [4] C. A. Baker, Y. M. Elyada, A. Parra, M. M. Bolton, *eLife* **2016**, *5*, e14193.
- [5] M. Dal Maschio, J. C. Donovan, T. O. Helmbrecht, H. Baier, *Neuron* **2017**, *94*, 774 e775.
- [6] W. Yang, L. Carrillo-Reid, Y. Bando, D. S. Peterka, R. Yuste, *eLife* **2018**, *7*, e32671.
- [7] Z. Zhang, L. E. Russell, A. M. Packer, O. M. Gauld, M. Häusser, *Nat. Methods* **2018**, *15*, 1037.
- [8] V. Nikolenko, B. O. Watson, R. Araya, A. Woodruff, D. S. Peterka, R. Yuste, *Front. Neural Circuits* **2008**, *2*, 5.
- [9] E. Papagiakoumou, V. de Sars, D. Oron, V. Emiliani, *Opt. Express* **2008**, *16*, 22039.
- [10] L. Golan, I. Reutsky, N. Farah, S. Shoham, *J. Neural Eng.* **2009**, *6*, 066004.
- [11] E. Papagiakoumou, F. Anselmi, A. Bègue, V. de Sars, J. Glückstad, E. Y. Isacoff, V. Emiliani, *Nat. Methods* **2010**, *7*, 848.
- [12] N. C. Pégard, A. R. Mardinly, I. A. Oldenburg, S. Sridharan, L. Waller, H. Adesnik, *Nat. Commun.* **2017**, *8*, 1228.
- [13] O. A. Shemesh, D. Tanese, V. Zampini, C. Linghu, K. Piatkevich, E. Ronzitti, E. Papagiakoumou, E. S. Boyden, V. Emiliani, *Nat. Neurosci.* **2017**, *20*, 1796.
- [14] A. R. Mardinly, I. A. Oldenburg, N. C. Pégard, S. Sridharan, E. H. Lyall, K. Chesnov, S. G. Brohawn, L. Waller, H. Adesnik, *Nat. Neurosci.* **2018**, *21*, 881.
- [15] L. Carrillo-Reid, W. Yang, Y. Bando, D. S. Peterka, R. Yuste, *Science* **2016**, *353*, 691.
- [16] B. Sun, P. S. Salter, C. Roeder, A. Jesacher, J. Strauss, J. Heberle, M. Schmidt, M. J. Booth, *Light: Sci. Appl.* **2018**, *7*, 17117.
- [17] H. Dana, S. Shoham, *Opt. Express* **2011**, *19*, 4937.
- [18] H. Dana, N. Kruger, A. Ellman, S. Shoham, *Opt. Express* **2013**, *21*, 5677.
- [19] E. Papagiakoumou, A. Bègue, B. Leshem, O. Schwartz, B. M. Stell, J. Bradley, D. Oron, V. Emiliani, *Nat. Photonics* **2013**, *7*, 274.
- [20] A. L. Allegra Mascaro, I. Costantini, E. Margoni, G. Iannello, A. Bria, L. Sacconi, F. S. Pavone, *Biomed. Opt. Express* **2015**, *6*, 4483.
- [21] F. Xia, C. Wu, D. Sinefeld, B. Li, Y. Qin, C. Xu, *Biomed. Opt. Express* **2018**, *9*, 6545.
- [22] G. M. Lerman, J. V. Gill, D. Rinberg, S. Shoham, *bioRxiv* **2018**, 456764.
- [23] R. W. Gerchberg, W. O. Saxton, *Optik* **1972**, *35*, 237.
- [24] T. A. Pologruto, B. L. Sabatini, K. Svoboda, *Biomed. Eng. Online* **2003**, *2*, 13.
- [25] F. Helmchen, W. Denk, *Nat. Methods* **2005**, *2*, 932.
- [26] P. Theer, W. Denk, *J. Opt. Soc. Am. A* **2006**, *23*, 3139.
- [27] M. Wang, C. Wu, D. Sinefeld, B. Li, F. Xia, C. Xu, *Biomed. Opt. Express* **2018**, *9*, 3534.
- [28] G. L. Galiñanes, P. J. Marchand, R. Turcotte, S. Pellat, N. Ji, D. Huber, *Biomed. Opt. Express* **2018**, *9*, 3624.
- [29] T. Wang, D. G. Ouzounov, M. Wang, C. Xu, presented at *Optics in the Life Sciences Congress*, San Diego, CA, USA, April **2017**.
- [30] E. A. Pnevmatikakis, A. Giovannucci, *J. Neurosci. Methods* **2017**, *291*, 83.
- [31] A. Picot, S. Dominguez, C. Liu, I. W. Chen, D. Tanese, E. Ronzitti, P. Berto, E. Papagiakoumou, D. Oron, G. Tessier, B. C. Forget, V. Emiliani, *Cell Rep.* **2018**, *24*, 1243.
- [32] N. Accanto, C. Molinier, D. Tanese, E. Ronzitti, Z. L. Newman, C. Wyart, E. Isacoff, E. Papagiakoumou, V. Emiliani, *Optica* **2018**, *5*, 1478.